coatings

MDPI

Article

Geomicrobial Investigations of Colored Outer Coatings from an Ethiopian Rock Art Gallery

Ying-Li Wu [1], Federica Villa [2,*], Gianmarco Mugnai [2], Marina Gallinaro [3], Enza Elena Spinapolice [3] and Andrea Zerboni [1]

[1] Dipartimento di Scienze della Terra "A. Desio", Università degli Studi di Milano, 20133 Milan, Italy; ying.wu@unimi.it (Y.-L.W.); andrea.zerboni@unimi.it (A.Z.)
[2] Dipartimento di Scienze per gli Alimenti, la Nutrizione e l'Ambiente, Università degli Studi di Milano, 20133 Milan, Italy; gianmarco.mugnai@unimi.it
[3] Dipartimento di Scienze dell'Antichità, Sapienza Università di Roma, 00185 Rome, Italy; marina.gallinaro@uniroma1.it (M.G.); enzaelena.spinapolice@uniroma1.it (E.E.S.)
* Correspondence: federica.villa@unimi.it

Received: 24 April 2020; Accepted: 29 May 2020; Published: 31 May 2020

Abstract: The open rock shelter of Yabelo in Ethiopia hosts diverse Holocene paintings of great cultural importance. The paintings are characterized by the presence of different mineral coatings, whose features have not been studied yet. Our goal was to understand whether different rock samples from the Yabelo paintings collected in close proximity may reveal coatings with different minerology and biology. Thus, elemental analyses combined with microscopic and molecular investigations were performed on two coatings, one whitish (sample 1) and one reddish (sample 2). Although both samples were dominated by heterotrophic bacteria, the two coatings showed distinct mineralogical and microbiological characteristics. Sample 1 contained higher amounts of Ca and P than sample 2, which was likely related to the presence of organic matter. Sample 1 hosted bacterial genera that are potentially involved in biomineralization processes, metal redox cycles and metal resistance. In contrast, sample 2 showed mainly pathogenic and commensal bacteria that are characteristic of animal and human microbiota, and other microorganisms that are involved in nitrogen and metal biogeochemical cycles. Overall, our results indicated that the bacterial communities were particular to the coating mineralogy, suggesting a potential role of the biological components in the crust genesis.

Keywords: bacterial community; rock art; rock coating; SEM-EDS; subaerial biofilms; CLSM; 16S rRNA gene sequencing

1. Introduction

Rock art is a fragile cultural heritage that requires conservation and proper methodological approaches to understand its state of preservation [1,2]. In fact, rock art—both in forms of paintings and petroglyphs—is subject to physical, biological and geochemical changes in the natural environment [3]. Mineral coatings covering large portions of the paintings and engravings are all too familiar to anyone who has looked closely at a rock art. Examples of these coatings are natural formations of calcium oxalate crusts [4,5], calcium carbonate layers [6,7], manganese-iron oxide deposits [8] and other mineral accretions [9] that may overlap and hide motifs and symbols of ancient rock paintings. Although the study of rock coatings has important implications in several fields, mineral depositions on rock art have been scarcely investigated, and their mechanisms of formation are still under investigation. Furthermore, limited information is available regarding the composition of the epilithic bacterial communities inhabiting the mineral coatings associated with prehistoric paintings, although the geoactive role of microorganisms has been well established [10,11]. Complex

microbial communities are embedded in a self-produced extracellular polymeric matrix (EPM) growth in the form of biofilms [11]. Biofilms can participate in rock varnish genesis [12,13], mineral formations in calcitic cave speleothems [14], sulfate deposit formation [15] and acid-mine drainage deposits [16].

Dorn [4] suggested that to understand the weathering and stabilization of rock art, it is important to study rock coatings; however, their contribution to the biodeterioration or bioprotection of rock art is still controversial. For instance, rock varnish in arid lands is a type of rock weathering that contributes to surface stabilization, thus hampering the effects of physical disaggregation [17–19].

The Yabelo area (Borana Zone, Oromia, southern Ethiopia) hosts diverse Holocene paintings of outstanding cultural importance. For many years these prehistoric paintings have been largely ignored by scholars, local communities and local authorities in charge of cultural heritage management. The paintings and rock surface are severely affected by deterioration processes causing loss of pigments, exfoliation, and the formation of different coatings as well as severe cracks [20]. Paintings and engravings are widespread, both in rock shelters and not-sheltered rock walls (open-air sites), often located in remote places that are currently inhabited by communities of different ethnic groups. The rock art in East Africa has been mainly studied focusing on two major aspects, namely chronology and stylistic interpretations. Only recently did scholars propose to study this rock art in a multidisciplinary approach involving archaeology and ethnography to help reconstruct the past, especially the emergence of pastoralism in this region [20].

Besides the archaeological context of African rock art, the characterization of the mineral coatings associated with the prehistoric paintings is needed to assess their putative role in the preservation or deterioration of the raw materials and pigments used. Furthermore, there are many open questions regarding the biological and mineralogical features of different colored outer coatings from the same bulk rock.

Our hypothesis is that coating types associated with the Yabelo paintings may show different chemical and biological compositions, despite being exposed to the same environment. In fact, the host rock provides the same moisture sources with the same chemical content to the rock coatings. Since the parental rock and the environmental exposure are the same, the contribution of microbial activities to the coatings' genesis should be considered. Thus, our goal was to understand whether different rock samples from the Yabelo paintings collected in close proximity may reveal coatings with different minerology and biology.

To this end, an integrated approach involving high-throughput sequencing and rock surface analyses was applied to investigate the bacterial diversity of two different pigmented areas close to the prehistoric paintings belonging to the same rock shelter. By sampling two different colored coatings from the same bulk rock, we were able to investigate how different patinas in close proximity may host different microbiota and, consequently, offer different biogeochemical processes. This research provides a novel combination of detailed microscopic images of the biofilm on the mineral surface coupled with analysis of chemical elements and DNA sequencing of microbial communities, which will be a new way of comprehending rock art preservation. This research is, to our knowledge, the first microbial investigation on African rock art.

2. Materials and Methods

2.1. Site Description and Sampling

The regional focus of this study is in East Africa, where recent archaeological investigation in southern Ethiopia confirmed that the rock art of the Yabelo region is of great cultural significance and requires further research as well as preservation [20,21]. The rock shelter YAB6 named by Hundie [22] opens along the cliff of a hill consisting of poorly to moderately metamorphosed granite. The hill is approximately 2 km northwest of the town Yabelo and referred to locally as Dhaka Kura (Crow's Rock) (Figure 1a). Paintings were identified, including cattle, wild animals and geometric shapes (Figure 1b). The pigments are vanishing, and the rock surface suffers exfoliation, as well as the

formation of red and white crusts or patinas. Direct anthropic damage was not detected, but local herders used and still use the rock shelter for grazing [20].

Several samples were taken from the shelter with chisels to investigate the many categories of rock weathering, crusts/patinas formation and pigments. Among them, we selected two samples representative of the two most common coatings present on the rock wall at YAB6, and from the most problematic panels in terms of conservation. These panels also present a high concentration of paintings; for the sake of heritage conservation, we collected samples at the margin of panels, far from paintings. The results of multiple analyses on two of these samples are reported here: sample 1 was a piece of exfoliating rock close to the bottom of the rock art panel with whitish patina overrunning the surface (Figure 1c); sample 2 was taken from the lower right with red patina on the surface (Figure 1d). Samples were collected by using sterile tools (mostly small chisels and lancets) and stored in sterile containers. Samples for DNA investigations were stored in sterile falcon tubes containing the stabilization solution DNA/RNA Shield (Zymo Research) to preserves the genetic integrity at ambient temperatures.

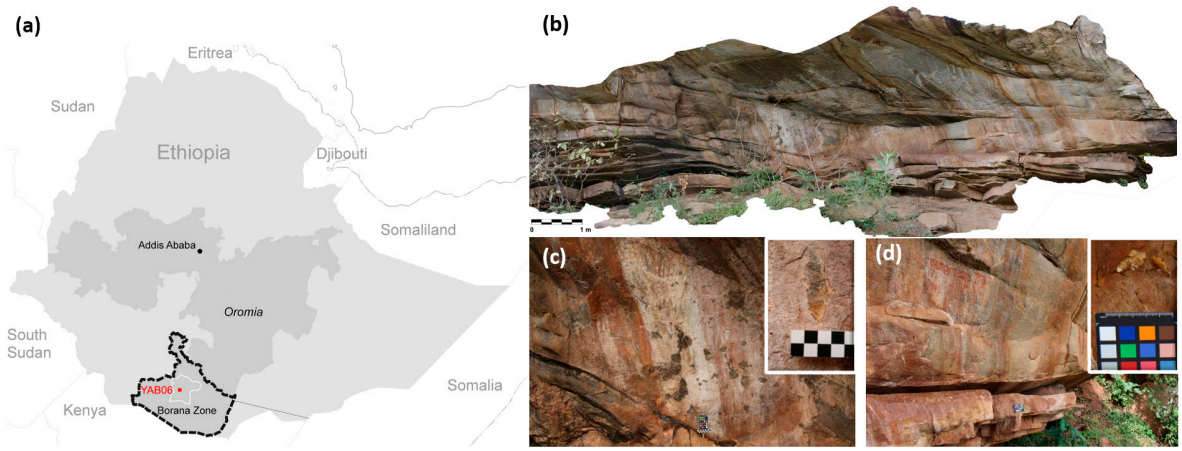

Figure 1. (**a**) Position of the Yabelo site; (**b**) overview of the rock art gallery of YAB6; (**c**) sample 1 was taken from white colored coatings close to the middle of the gallery; (**d**) sample 2 was taken from red colored coatings at the lower right.

2.2. Microscopic Characterization of the Rock Substrate and Mineral Coating

Samples were cut perpendicularly to the surface and polished into thin sections mounted on glass slides according to the protocol described in [19], in order to investigate the effects of weathering. Micromorphology of weathering of thin sections [23] was examined with an optical petrographic microscope (OPTIKA B-1000 POL, Ponteranica, Bergamo, Italy) under plane-polarized light (PPL) and cross-polarized light (XPL). Afterwards the thin sections were carbon coated and observed with a Scanning Electron Microscope (SEM, JEOL JSM-IT500) (JEOL Ltd., Tokyo, Japan) coupled with energy dispersive X-ray spectrometry (EDS) for chemical characterization with accelerating voltage 20 kV. All measurement data normalized to 100 weight % oxide.

2.3. Visualization of Biofilm Structure

Surface crusts from the rock samples were taken by using adhesive tapes (Fungi-tape, Fisher scientific) and observed with a Confocal Laser Scanning Microscope (CLSM) (Nikon, Amsterdam, Netherlands) in both fluorescence and reflection modes. Confocal images were collected using a Nikon A1 laser scanning confocal microscope and a 20×/0.75 numerical aperture Plan Apo λ (Nikon, Amsterdam, Netherlands) objective with a working distance of 1 mm. Captured images were analyzed with the software NIS-Elements by Nikon (Nikon, Amsterdam, Netherlands) for the 3D reconstructions of the biofilms. The reflection mode (excitation 488 nm) records the mineral surface of the lithic sample. Autofluorescence from phototrophic pigments was assigned to the blue channel

and collected using the 633 nm laser line in the emission range of 663–738 nm. Biofilm components were visualized after fluorescent staining. SYTO® 9 (excitation 485 nm/498 nm, BacLight™ ThermoFisher, Milan, Italy) labelled nucleic acids and emitted green fluorescence. For its acquisition the 488 nm laser line and the 500–550 nm emission filter were used. Polysaccharide components of the EPM were labelled with Concanavalin-A-Texas red (excitation 561 nm/emission 570–620 nm).

2.4. DNA Extraction and Sequencing

Rock samples, conserved in the stabilization solution DNA/RNA Shield (Zymo Research), were processed a few days after their collection. Total genomic DNA were extracted according to the manufacturer's instructions of PowerBiofilm DNA Isolation Kit (MoBio Laboratories Inc., Carlsbad, CA, USA). High-throughput sequencing analysis of the V3–V4 region of the bacterial 16S rRNA gene (primers CS1_341F/CS2_806R) was performed by using a MiSeq platform (Illumina) with v3 chemistry providing 2 x 300 paired-end reads [24]. Raw data were pre-processed, quality filtered, trimmed, de-noised, paired, and modelled via QIIME2 [25] and DADA2. Chimeras were detected using DADA2 according to the "consensus" method [26]. Sequences were clustered into Amplicon Sequences Variants (ASV). ASVs were assigned using a Naïve-Bayes classifier trained on the SILVA database [27]. Multi packages of R software (R Core Team, Version 3.3.0, Vienna, Austria) [28] were used to calculate the alpha diversity, to generate the rarefaction curves and the Venn diagram. Samples were rarefied at the minimum library size of 92,380. The rarefaction curves were drawn using the function "rarefaction" [29] from the vegan R-package [30].

3. Results

3.1. Optical Microscopy and SEM-EDS Analysis

Thin section of sample 1 under PPL showed a dark coating growing along the lithic surface and extending into cracks of the rock substrate with reddish organic substances (Figure 2a). Under higher magnification (in PPL and XPL) the coatings appeared brownish, and in XPL there were some small bright (birefringent) crystals (Figure 2c,d). SEM images in back scattering electron mode from sample 1 revealed a continuous layer of mineral coating that was 10–20 μm thick and exceeded 30 μm in certain locations. The coating grew on the silicate-bearing surface of the substrate and it was more developed for instance in correspondence with an iron oxides inclusion (Figure 3a). SEM-EDS analysis suggested the coating is mainly quartz and clay minerals, being enriched in Si, Al, Mg, and K (Table 1). In the thicker coating that grew inside the cavity of the iron-rich inclusion (Figure 3a), the amount of P_2O_5 (25%–33%) and CaO (33%–41%) increased from the bottom of the cavity towards the opening, but at the surface they were reduced (P_2O_5 7.73%, CaO 13.43%) and replaced by higher SiO_2. The amount of FeO in this cavity remains in the range of 1%-6% (Table 1). At another location (Figure 3b), the surface coatings contained higher amounts of P_2O_5 (6%–16%), CaO (9%–19%) and FeO (4%–13%) than the underlying mineral that is mostly SiO_2 (52%), Al_2O_3 (15%) and K_2O (11%). Other examples of thick coatings (Figure 3c) that contain high amounts of P_2O_5 (25.11%, 14.64%) and CaO (31.97%, 13.75%) are shown in Table 1. Such parts of the coatings have more complex layers including a layer of clay minerals and a layer of iron and calcium phosphates.

The outer surface of sample 2 also showed a dark coating under the petrographic microscope (PPL), with some organic matter caught in crevices (Figure 2b). In XPL there were also some tiny bright crystals in the otherwise brown coating. Images generated from back scattering electrons from SEM showed the inorganic part of the coating to be 10–20 μm thick, thinner than sample 1 in general (Figure 3d). SEM-EDS analyses revealed most of the coating to be silicate and clay minerals, but in a few spot analyses there were slightly higher amounts of CaO (2%–15%) and FeO (2%–7%), while P_2O_5 (1%–5%) was significantly lower than in sample 1 (Table 1).

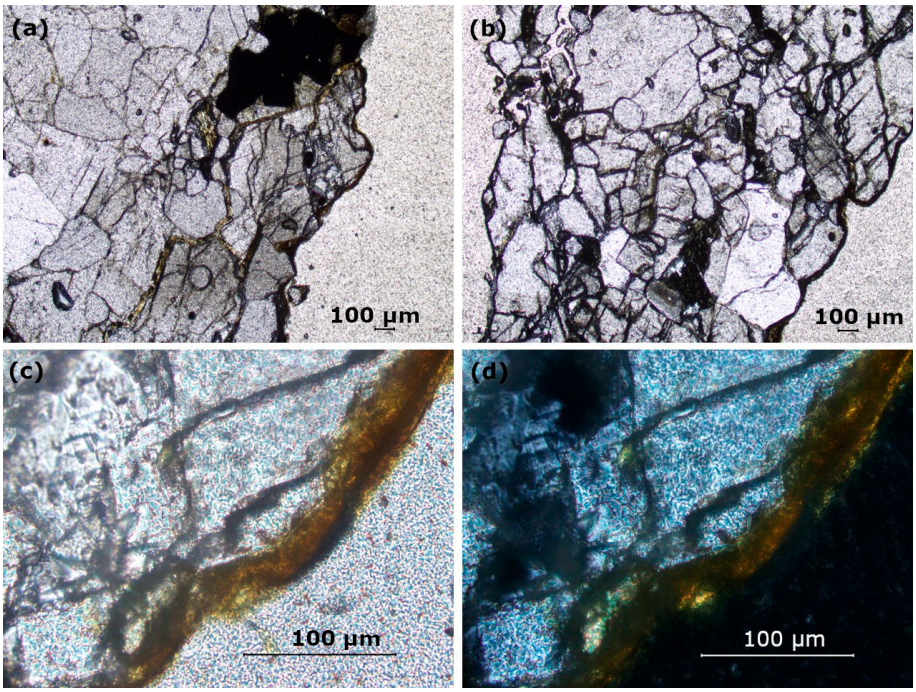

Figure 2. (**a**) Plane-polarized light (PPL) microscopic image showing black coating growing on the lithic surface of sample 1 and extending into cracks, the iron inclusion is black; (**b**) PPL microscopic image showing black coating growing on the lithic surface of sample 2; (**c**) higher magnification of the coating from sample 1 in PPL and (**d**) in cross-polarized light (XPL).

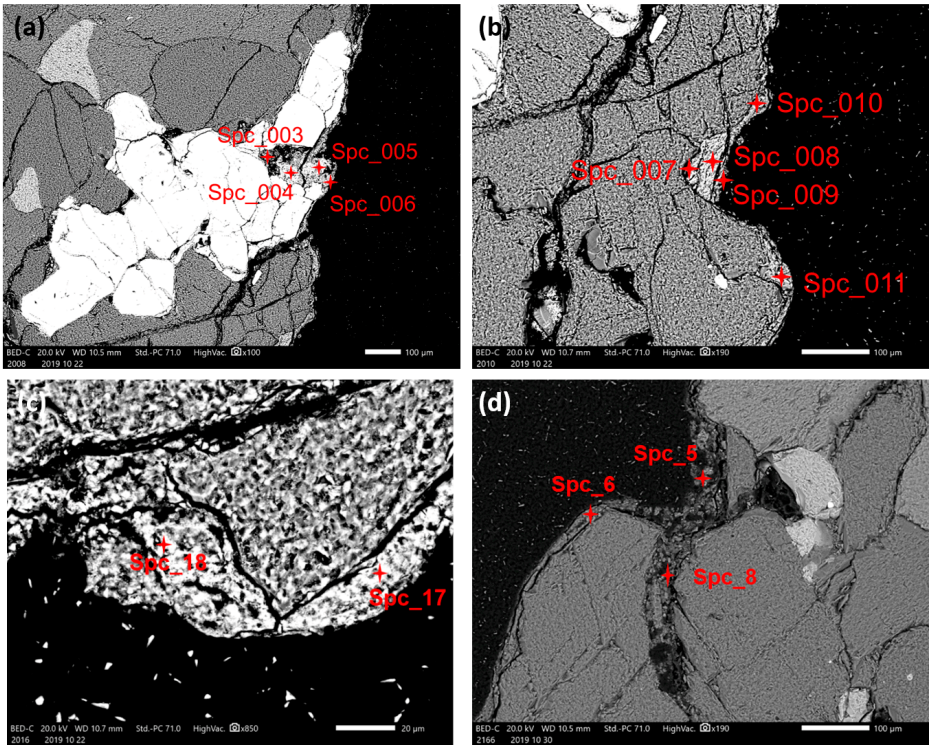

Figure 3. (**a**) Backscattered electron images in SEM showing the iron inclusion in rock sample 1 as white reveal a continuous inorganic coating; (**b**) site indications of EDS analyses of coatings on sample 1; (**c**) site indications of EDS analyses of coatings on sample 1; (**d**) backscattered electron images in SEM of sample 2 with inorganic coating and sites of EDS analyses.

Table 1. EDS analyses of coatings from sample 1 and 2. All measurement data normalized to 100 weight % oxides, not all elements are shown. n.d. = not detected.

		SiO_2	Al_2O_3	FeO	CaO	MgO	P_2O_5	SO_3	K_2O
Sample 1	Spc_003	3.45	1.01	1.21	33.93	5.03	25.47	1.53	0.84
Sample 1	Spc_004	5.22	0.77	6.60	36.99	2.72	29.57	0.76	0.69
Sample 1	Spc_005	3.44	0.55	1.97	41.13	2.00	33.62	0.75	n.d.
Sample 1	Spc_006	23.44	9.58	5.22	13.43	4.26	7.73	0.46	1.52
Sample 1	Spc_007	52.20	15.08	n.d.	n.d.	n.d.	n.d.	n.d.	11.45
Sample 1	Spc_008	52.64	15.28	n.d.	n.d.	n.d.	n.d.	n.d.	11.51
Sample 1	Spc_009	14.37	6.56	4.37	19.99	4.57	16.00	1.05	1.08
Sample 1	Spc_010	28.35	5.76	13.18	9.33	4.22	7.64	0.53	2.33
Sample 1	Spc_011	28.95	12.66	6.25	10.04	7.13	6.26	0.59	2.86
Sample 1	Spc_17	13.19	5.68	2.11	31.97	3.92	25.11	0.56	0.89
Sample 1	Spc_18	27.01	14.85	4.44	13.75	n.d.	14.64	n.d.	2.05
Sample 2	Spc_5	38.77	14.05	7.42	2.39	2.34	0.98	0.32	2.31
Sample 2	Spc_6	21.45	9.94	5.44	15.97	2.61	5.54	0.51	1.92
Sample 2	Spc_8	19.55	16.64	2.00	10.78	n.d.	2.29	n.d.	0.92

3.2. Biofilm Characterization

Figure 4 showed the reconstructed 3D biofilm images from confocal images with the software NIS-Elements by Nikon. Sample 1 had coccoid aggregates of photosynthetic bacteria dispersed sporadically on the higher part of the sample, and smaller clusters of chemotrophs colonizing the whole rock surface evenly. Spaces between the phototrophs and chemotrophs appeared to be covered in a monolayer of extracellular polysaccharides. Together these components constituted a dynamic biofilm that covered the whole surface of sample 1, with phototrophic and chemotrophic communities embedded in a continuous layer of polysaccharide matrix.

In comparison, sample 2 had a less dense biofilm coverage. Congregates of chemotrophs differing in size grew on most of the lithic surface, concentrating on the ridges and exempting voids or smooth mineral surfaces. Faint traces of polysaccharides could be seen through some of the chemotrophs. In general, neither phototrophs nor fungal structures were observed on sample 2. As a result, sample 1 presented a more diverse biofilm with higher phototrophs, chemotrophs and the EPM than sample 2.

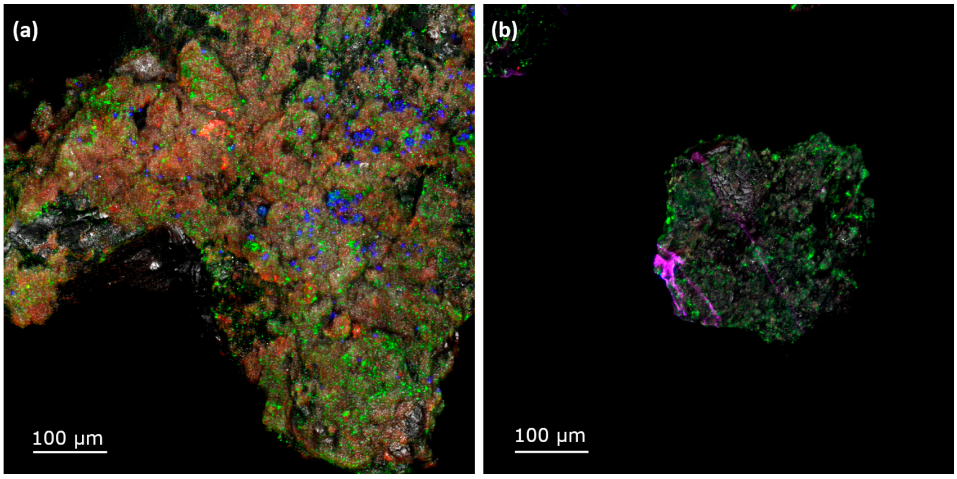

Figure 4. Confocal microscope images of biofilms on (**a**) Sample 1 and (**b**) Sample 2. Color key: phototrophs, blue (autofluorescence); chemotrophs, green (SYTO 9); polysaccharides, red (Con A); stone, gray (reflection).

3.3. Bacterial Communities

The 16S rRNA data set consisted of 186,517 reads clustered in 173 ASVs. The rarefaction curves showed that sequencing depth was sufficient for a thorough description of the bacterial communities (Figure 5a). According to the Venn diagram only 2 ASVs were shared between the two samples, where 139 species were unique to sample 1 and 32 species were unique to sample 2, showing differences between the bacterial communities (Figure 5b). Two species that were common for both samples are: *Curvibacter* and *Undibacterium*, belonged to the *Burkholderiaceae* family. Alpha-diversity indices indicated that the diversity level of bacterial community was higher in sample 1 than in sample 2 (Table 2).

Ten bacterial phyla, 18 classes, 36 orders, 56 families and 59 genera were detected overall (Figure 6). Sample 1 was dominated by Firmicutes (77.17%) and Proteobacteria (8.75%), with notable percentages of Actinobacteria (8.06%), Cyanobacteria (2.94%) and Acidobacteria (1.76%). At genus level, the core microbiome of sample 1 was mainly composed of *Bacillus* (Firmicutes, Bacilli, Bacillales, Bacillaceae, 21.58%), *Streptococcus* (Firmicutes, Bacilli, Lactobacillales, Streptococcaceae, 20.81%), *Staphylococcus* (Firmicutes, Bacilli, Bacillales, Staphylococcaceae, 17.34%) and *Paenibacillus* (Firmicutes, Bacilli, Bacillales, Paenibacillaceae, 6.48%). Sample 2 consisted mainly of Firmicutes (66.77%) and Proteobacteria (33.07%), with the genera *Facklamia* (Firmicutes, Bacilli, Lactobacillales, Aerococcaceae, 48.05%), *Comamonas* (Proteobacteria, Betaproteobacteria, Burkholderiales, Comamonadaceae, 29.06%) and *Atopostipes* (Firmicutes, Bacilli, Lactobacillales, Carnobacteriaceae, 11.43%) the most abundant taxa.

After bibliographic research, the ASVs were classified according to eight main categories reported in Figure 7. The reads allocated to each category were presented as a heatmap to show the main features of the biofilm communities in samples 1 and 2. Inferred physiology showed the predominance of bacteria involved in mineral precipitation, metal redox cycle and metal resistance in sample 1, while microorganisms derived from animal and human sources and those involved in the biochemical cycle of elements, such as metal and nitrogen, were the signature of sample 2.

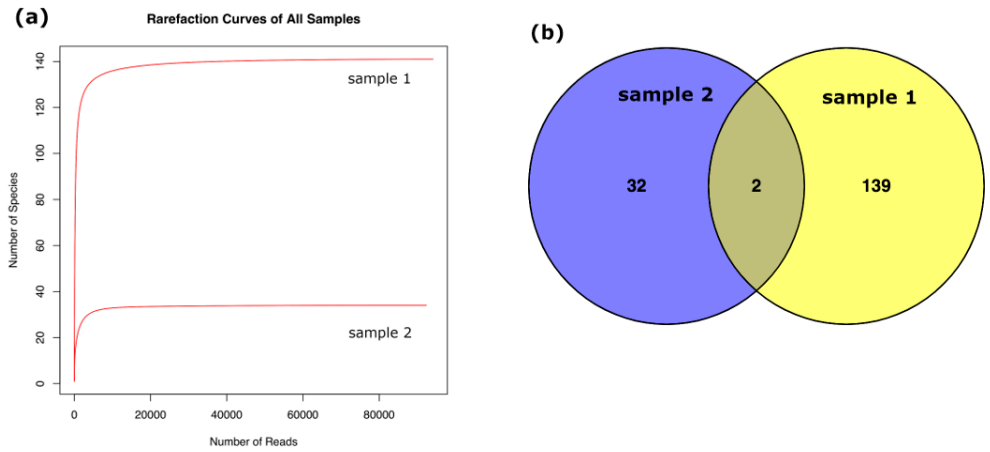

Figure 5. (**a**) Rarefaction curves for bacterial communities in sample 1 and sample 2; (**b**) Venn diagram drawn from number of amplicon sequences variants (ASVs) representative of sample 1 and sample 2.

Table 2. bacterial community richness and alpha-diversity indices.

Samples	Reads	Richness	Eveness	Shannon	Simpson
Sample 1	94137	141	0.60	4.26	0.02
Sample 2	92380	34	0.33	1.70	0.27

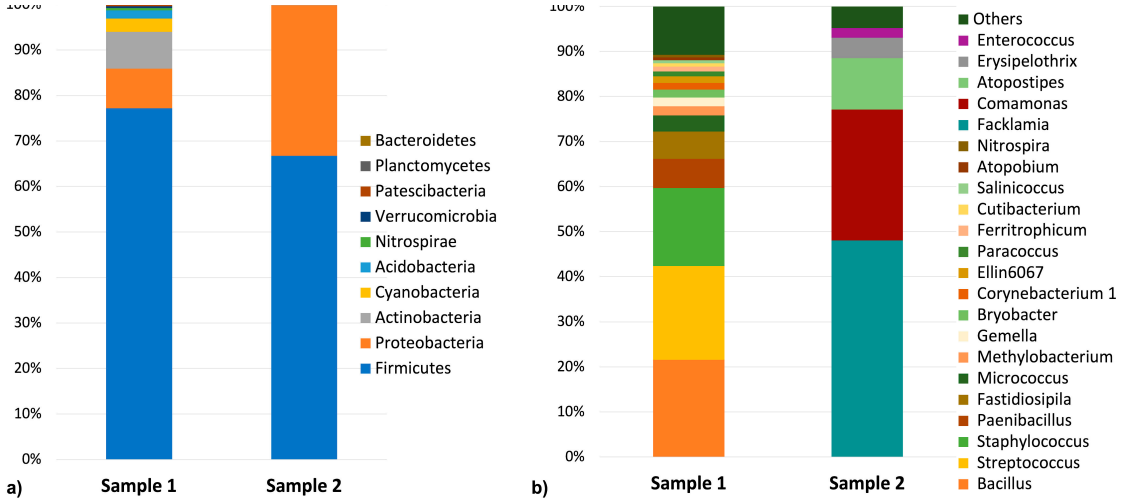

Figure 6. Metagenomic data of rock samples to (**a**) Phylum level; (**b**) Genus level with a relative abundance of higher than 1% in the samples.

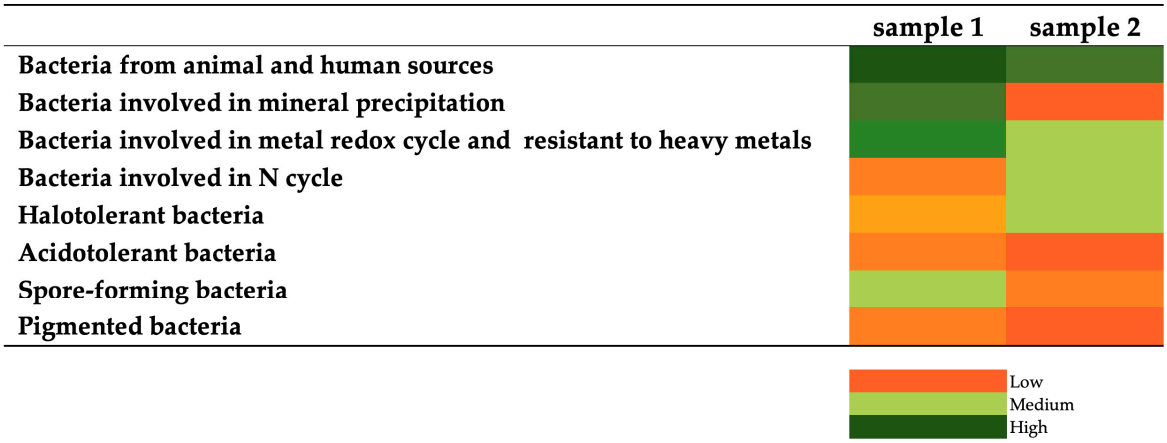

Figure 7. Heatmap representing the main features of the biofilm communities inhabiting the coating samples.

4. Discussion

There is an abundance of literature that highlights the cultural significance of rock art as well as the attempts to date paintings and petroglyphs in many parts of the world [31,32]. However, rock art is one of the most fragile forms of ancient heritage and its preservation is understudied. In particular, the nature and the role of mineral coatings covering rock paintings are poorly investigated. For instance, Zerboni et al. [33], discussed the preservation and dating of petroglyphs in the Sultanate of Oman, where a dark crust that preserved the grooves could be related to biological deposition. In Australia, Chalmin et al. [34] performed a geochemical analysis on microlayers of rock art surface, finding that the weathered rock layer contained Si, Al, K, P and Fe. Green et al. [9] observed four types of mineral depositions in Australian rock art sites, and identified sulphate, phosphate and calcium minerals. Krinsley et al. [35,36] used scanning electron microscope (SEM) and chemical characterization on Mn-rich biologically formed rock varnish in fast accreting moist environments. Lang-Yona et al. [37] performed a metagenomic analysis on desert varnish and discussed the indirect contribution of microorganisms to the varnish formation. However, outside the domain of rock varnish, there is a substantial lack of knowledge concerning the role of microorganisms in rock coatings development. Furthermore, little is known about whether different rock samples collected in close proximity on the same bulk rock may accommodate coatings with different minerology and biology. To answer this question, comprehensive research that combines the geochemical

characterization and the biofilm community investigation of these colored coatings retrieved from the rock art is necessary.

The SEM investigation revealed that rock coatings consists of layers of clay minerals, calcium-bearing minerals, phosphates- and iron-rich oxides–hydroxides. The formation of some of these mineral coatings can be related to some biological processes. Calcium-rich minerals in the form of oxalates are common secondary minerals formed by microbial mobilization, while iron-rich minerals have also been reported as a biological precipitation [38]. Calcium- and phosphate-rich coatings were reported on desert pavement cobbles [18,19] as a product of microbial activity or endolithobionts decay, and iron phosphate coatings have been found in stone coatings, where the iron is possibly from a bacterial precipitation [18,39]. Both scanning electron and optical microscopies showed that the coatings in sample 1 were thicker than sample 2. Moreover, chemical analyses of the coatings showed that sample 1 had higher amounts of Ca, P, and Fe than sample 2. The analysis demonstrated that coating types with different chemical compositions can still occur despite their close proximity to each other. Iron films and sulfate crusts have been found within a couple of meters from one another, a well-delineated phenomenon in the Yosemite Valley and in Kärkevagge, Swedish Lapland [40,41]. Since the different coatings are presumably exposed to the same physical and chemical macro environment, a possible biological origin of the colored coatings is considered.

To this end, the bacterial communities associated with two colored coatings from the Yabelo painting collected in close proximity were studied. From the confocal images, the biofilms of sample 1 were shown to be more developed and complex than those of sample 2. Overall, the taxonomic profiles detected in both samples were dominated by Firmicutes. In contrast, previous studies investigating the microbial communities associated with Palaeolithic art in caves reported an abundance of Proteobacteria, Actinobacteria, Acidobacteria and Cyanobacteria in the patinas [42–44]. At the phylum level, our findings are in line with those of Roldán [45], proving the similarity of the communities of our samples to the bacterial communities found in the prehistoric Spanish Levantine rock art and Atlanterra and La Graja shelters in Southern Spain [46,47].

The 16S rRNA gene sequencing analysis clearly indicated that the bacterial communities are particular to the coating mineralogy at genus level. The only two species shared by the samples are *Curvibacter*, which is involved in the precipitation of calcium carbonate [48], and *Undibacterium*, which is responsible for carbonate dissolution and Fe-oxyhydroxides [49]. A common feature between the two coating samples is the predominance of heterotrophic bacteria, which suggests that the most common energy-acquiring mechanism in the rock art system under investigation is relying on the organic compounds for nourishment. The dominance of heterotrophs may be derived from the organic materials generated by the human activities at the rock shelter and animal herding [20]. Despite the dominance of heterotrophs, the bacterial community in sample 1 also includes phototrophs and chemolithoautotrophs that use light and inorganic compounds to grow, respectively. The cyanobacteria identified in the sample 1 belongs to the class of Melainabacteria that is prevalent in the gut of herbivorous mammals and humans with a predominantly vegetarian diet [50]. The microaerobic and chemolithoautotrophic bacterium *Ferritrophicum* plays an important role in Fe cycling in many terrestrial and freshwater environments [51].

From the taxonomic assignment, the main futures of the community can be inferred, and the associations between the mineralizing metabolisms and the rock coating mineralogy can be obtained. Although the dominance of biomineralizing bacteria does not indicate whether these microorganisms are actively involved in the coating's origin, there is a clear relationship between the coating mineralogy and the bacterial community structures. In fact, the biofilm inhabiting the coating of sample 1 is mainly characterized by bacteria involved in mineral precipitation, metal redox cycle and metal resistance. Among the ASVs in sample 1, the dominant genera are *Bacillus, Streptococcus,* and *Staphylococcus*. *Bacillus* was associated with carbonate precipitation of speleothem formations in Tjuv-Ante's Cave, Northern Sweden [52]. *Bacillus* strains were also involved in the biofilm formation and calcite binding because of their EPM production capability [53]. *Bacillus* is also the most important calcium-carbonate biomineralization bacteria that has an industrial application ranging from the CO_2 sequestration to reduce atmospheric CO_2, to the rescue of historical buildings. Bacterial

biomineralization has been reported by Konhauser and Riding [54] and the ability of *Bacillus* to precipitate calcium carbonates was studied for its impact on built heritage, for instance on rock monument surfaces [55], and even tested as a potential bioconsolidating agent for monumental stones [56–58]. Furthermore, Gonzalez et al. [46] isolated a number of iron reducing *Bacillus* strains from rock paintings based on the red iron oxides in a sandstone shelter in Spain. Fishman et al. [59] reported that the calcium-phosphate-based mineral apatite is created via the biomineralization by a large number of bacteria including *Streptococcus* and *Corynebacterium*, which are the strains identified in sample 1. Although Adetutu et al. [60] considered *Staphylococcus* as an indicator of the human interaction in the open shelters, the bacterium can also precipitate carbonates [61] and can be involved in Hg, Fe(III) reduction [62]. Thus, the biomineralization processes in sample 1 are primarily driven by the heterotrophic communities that alter the local condition to promote the mineral precipitation [63,64]. *Acinetobacter* and *Arthrobacter* are both involved in Cr(VI) and Mn(IV) reduction [62]. At the genus level, a large number of metal-resistance bacteria in sample 1 were observed, including the species of *Corynebacterium*, *Bryobacter*, *Gemella* and *Methylobacterium* [62,65–67].

Bacteria from animals and humans and those involved in the biochemical cycle of elements such as metal and nitrogen, are the signature of a biofilm inhabiting the coating of sample 2. In fact, species of the genus *Facklamia* are associated with warm-blooded animals, including the gut system of pigs [68] and the urinogenital tract of female cows, where the bacterium may cause an opportunistic infection [69]. *Erysipelothrix*, facultative spore-forming Gram-positive bacilli, can cause a wide range of diseases in a variety of species such as sheep, poultry, cattle and humans [70]. *Comamonas* is a halotolerant, saprotrophic bacterium routinely found in oligotrophic environments (like rock surfaces and cave environments), capable of degrading a number of nitrogen-containing aromatic compounds while releasing usable nitrate and ammonia [71]. *Atopostipes,* previously isolated from swine manure [72], was the predominant bacterium in chicken litters that is responsible for odor production [73]. *Enterococcus* is a lactic acid bacterium comprising both pathogenic and commensal species ubiquitous in various environments including the gut system. Due to its tolerance to salts and acids, strains of *Enterococcus* spp. are highly competitive and adaptable to several ecosystems including lithic environments [45,74]. In addition, several members of *Enterococcus* genus have been reported to produce bacteriocins, which are antimicrobial compounds that contribute to either the stability or the dynamics of the microbial communities [75].

5. Conclusions

For the first time, a mineralogical characterization is combined with a microbial characterization to study the different coatings on an African rock art site. The results demonstrated the following conclusions:

- The two coatings show distinct features, where the coating in sample 1 contains higher amounts of Ca and P than that of sample 2, which is likely related to the presence of organic matter.
- Heterotrophism is the most common energy-acquiring mechanism shared between the two coating communities. The widespread distribution of heterotrophic bacteria is likely to be derived from animal and human sources, which also provide important sources of organic materials generated by the herding activities around the rock art shelter.
- The core bacterial community of sample 1 is substantially different from sample 2, indicating that the microbiota is unique to the coating minerals. In fact, sample 1—the coating with the highest Fe, Ca and P content—hosts bacterial genera that are potentially involved in biomineralization processes, metal redox cycles and metal resistance. In contrast, sample 2 shows mainly pathogenic and commensal bacteria that are characteristic of the animal and human microbiota, and other microorganisms that are involved in nitrogen and metal biogeochemical cycles.

Unveiling the composition of the microbial communities in the coatings of prehistoric paintings has important implications for the conservation strategy. In future work, the coating minerals will be precisely identified using X-ray powder diffraction (XRD) analysis, while the role of the active

bacterial community in coating genesis and rock art protection or biodeterioration will be deciphered using the RNA-based analysis.

Author Contributions: Conceptualization, F.V., M.G., and A.Z.; molecular and chemical analysis, Y.W.; bioinformatic investigations, G.M.; sample acquisition, M.G. and E.E.S.; writing—original draft preparation, Y.W., G.M., and M.G.; writing—review and editing, F.V. and A.Z. All authors have read and agreed to the published version of the manuscript.

Funding: Fieldwork in Ethiopia was supported by the (H)ORIGN Project, funded by the Italian Ministry of Education, University, and Research (MIUR) within the framework of the SIR 2014 program (Project RBSI142SRD, PI: E.E.S.). Part of this research was supported by the Italian Ministry of Education, University, and Research (MIUR) through the project "Dipartimenti di Eccellenza 2018–2022" (WP4–Risorse del Patrimonio Culturale) awarded to the Dipartimento di Scienze della Terra "A. Desio" of the Università degli Studi di Milano. The PhD of Ying-Li Wu is granted by the Ministry of Education, Taiwan.

Acknowledgments: Field missions to Ethiopia are part of the project "Tracing the First Herders in East Africa: Cultural, Symbolic and Biological Trajectories" (permit n.14/2006) directed by Marina Gallinaro. The Authority for Research and Conservation of Cultural Heritage (Addis Ababa) granted to MG all necessary permits for sampling, exportation, and analyses of samples described in the study, which complied with all the applicable regulations. We thank the Authority for Research and Conservation of Cultural Heritage (Addis Ababa), the Italian Ministry for Foreign Affairs, the Italian Institute of Culture in Addis Ababa, and the Borana Zone Culture and Tourism Office. We thank Martina Mervic for preparing DNA samples and Stefania Crespi for preparing and assisting SEM analyses.

Conflicts of Interest: The authors declare no conflict of interest.

References

1. Whitley, D.S. *Introduction to Rock Art Research*, 2nd ed.; Informa UK Limited: Colchester, UK, 2011.
2. Darvill, T. *Open-Air Rock-Art Conservation and Management*; Routledge: Abingdon-on-Thames, UK, 2014.
3. Dorn, R. 4.5 Rock Coatings. In *Treatise on Geomorphology*; Elsevier BV: Amsterdam, The Netherlands, 2013; Volume 4, pp. 70–97.
4. Hernanz, A.; Ruiz, J.F.; Madariaga, J.M.; Gavrilenko, E.; Maguregui, M.; De Vallejuelo, S.F.-O.; Martinez-Arkarazo, I.; Alloza-Izquierdo, R.; Baldellou-Martínez, V.; Viñas-Vallverdú, R.; et al. Spectroscopic characterisation of crusts interstratified with prehistoric paintings preserved in open-air rock art shelters. *J. Raman Spectrosc.* **2014**, *45*, 1236–1243, doi:10.1002/jrs.4535.
5. Roberts, A.; Campbell, I.; Pring, A.; Bell, G.; Watchman, A.; Popelka-Filcoff, R.; Lenehan, C.; Gibson, C.; Franklin, N. A multidisciplinary investigation of a rock coating at Ngaut Ngaut (Devon Downs), South Australia. *Aust. Archaeol.* **2015**, *80*, 32–39, doi:10.1080/03122417.2015.11682042.
6. Rousaki, A.; Vargas, E.; Vázquez, C.; Aldazábal, V.; Bellelli, C.; Calatayud, M.C.; Hajduk, A.; Palacios, Òscar; Moens, L.; Vandenabeele, P. On-field Raman spectroscopy of Patagonian prehistoric rock art: Pigments, alteration products and substrata. *TrAC Trends Anal. Chem.* **2018**, *105*, 338–351, doi:10.1016/j.trac.2018.05.011.
7. Mauran, G.; Lebon, M.; Détroit, F.; Caron, B.; Nankela, A.; Pleurdeau, D.; Bahain, J.-J. First in situ pXRF analyses of rock paintings in Erongo, Namibia: Results, current limits, and prospects. *Archaeol. Anthr. Sci.* **2019**, *11*, 4123–4145, doi:10.1007/s12520-019-00787-7.
8. Šebela, S.; Miler, M.; Skobe, S.; Torkar, S.; Zupančič, N. Characterization of black deposits in karst caves, examples from Slovenia. *Facies* **2015**, *61*, 6, doi:10.1007/s10347-015-0430-z.
9. Green, H.; Gleadow, A.; Finch, D.; Hergt, J.M.; Ouzman, S. Mineral deposition systems at rock art sites, Kimberley, Northern Australia — Field observations. *J. Archaeol. Sci. Rep.* **2017**, *14*, 340–352, doi:10.1016/j.jasrep.2017.06.009.
10. Gadd, G.M. Metals, minerals and microbes: Geomicrobiology and bioremediation. *Microbiology* **2009**, *156*, 609–643, doi:10.1099/mic.0.037143-0.
11. Villa, F.; Cappitelli, F. The Ecology of Subaerial Biofilms in Dry and Inhospitable Terrestrial Environments. *Microorganisms* **2019**, *7*, 380, doi:10.3390/microorganisms7100380.

12. Kuhlman, K.R.; Fusco, W.G.; La Duc, M.T.; Allenbach, L.B.; Ball, C.L.; Kuhlman, G.M.; Anderson, R.C.; Erickson, I.K.; Stuecker, T.; Benardini, J.; et al. Diversity of Microorganisms within Rock Varnish in the Whipple Mountains, California. *Appl. Environ. Microbiol.* **2006**, *72*, 1708–1715, doi:10.1128/aem.72.2.1708-1715.2006.
13. Esposito, A.; Ahmed, E.; Ciccazzo, S.; Sikorski, J.; Overmann, J.; Holmström, S.J.M.; Brusetti, L. Comparison of Rock Varnish Bacterial Communities with Surrounding Non-Varnished Rock Surfaces: Taxon-Specific Analysis and Morphological Description. *Microb. Ecol.* **2015**, *70*, 741–750, doi:10.1007/s00248-015-0617-4.
14. Mistri, A.; Mukherjee, A.; Watkin, E.L.J. Microbial Diversity and Mineralogical-Mechanical Properties of Calcitic Cave Speleothems in Natural and in Vitro Biomineralization Conditions. *Front. Microbiol.* **2018**, *9*, 40, doi:10.3389/fmicb.2018.00040.
15. Bostick, B.C. Massive ore deposits from microscopic organisms. *Geology* **2019**, *47*, 191–192, doi:10.1130/focus022019.1.
16. Meier, J.; Piva, A.; Fortin, D. Enrichment of sulfate-reducing bacteria and resulting mineral formation in media mimicking pore water metal ion concentrations and pH conditions of acidic pit lakes. *FEMS Microbiol. Ecol.* **2011**, *79*, 69–84, doi:10.1111/j.1574-6941.2011.01199.x.
17. Dorn, R.I. Desert Rock Coatings. In *Geomorphology of Desert Environments*; Springer Science and Business Media LLC: Berlin/Heidelberg, Germany, 2009; pp. 153–186.
18. Dorn, R.I. *Rock Coatings*; Elsevier Science: Amsterdam, The Netherlands, 1998.
19. Zerboni, A. Holocene rock varnish on the Messak plateau (Libyan Sahara): Chronology of weathering processes. *Geomorphology* **2008**, *102*, 640–651, doi:10.1016/j.geomorph.2008.06.010.
20. Gallinaro, M.; Zerboni, A.; Solomon, T.; Spinapolice, E.E. Rock Art between Preservation, Research and Sustainable Development—A Perspective from Southern Ethiopia. *Afr. Archaeol. Rev.* **2018**, *35*, 211–223, doi:10.1007/s10437-018-9289-z.
21. Spinapolice, E.E.; Gallinaro, M.; Zerboni, A. New investigations in Southern Ethiopia (Yabelo and Gotera): Pleistocene and Holocene archaeological evidences. *Scienze Dell'Antichità* **2017**, *23*, 37–47.
22. Hundie, G. The Emergence of Prehistoric Pastoralism in Southern ETHIOPIA. Ph.D. Thesis, University of Florida, Gainesville, FL, USA, 2001.
23. Cremaschi, M.; Trombino, L.; Zerboni, A. *Palaeosoils and Relict Soils*; Elsevier BV: Amsterdam, The Netherlands, 2018; pp. 863–894.
24. Rapin, A.; Pattaroni, C.; Marsland, B.J.; Harris, N.L. Microbiota analysis using an illumina MiSeq platform tosequence 16S rRNA genes. *Curr. Protoc. Mouse Biol*. **2017**, *7*, 100–129.
25. Bolyen, E.; Rideout, J.R.; Dillon, M.R.; Bokulich, N.A.; Abnet, C.C.; Al-Ghalith, G.A.; Alexander, H.; Alm, E.J.; Arumugam, M.; Asnicar, F.; et al. Reproducible, interactive, scalable and extensible microbiome data science using QIIME 2. *Nat. Biotechnol.* **2019**, *37*, 852–857.
26. Callahan, B.J.; McMurdie, P.; Rosen, M.J.; Han, A.W.; Johnson, A.J.; Holmes, S. DADA2: High-resolution sample inference from Illumina amplicon data. *Nat. Methods* **2016**, *13*, 581–583, doi:10.1038/nmeth.3869.
27. Quast, C.; Pruesse, E.; Yilmaz, P.; Gerken, J.; Schweer, T.; Yarza, P.; Peplies, J.; Glöckner, F.O. The SILVA ribosomal RNA gene database project: Improved data processing and web-based tools. *Nucleic Acids Res.* **2012**, *41*, D590–D596, doi:10.1093/nar/gks1219.
28. R Core Team. *R: A Language and Environment for Statistical Computing*; R Foundation for Statistical Computing: Vienna, Austria, 2013. Available online: http://www.r-project.org/ (accessed on November 2019).
29. Jacobs, J. Individual Based Rarefaction in R [online]. 2012. Available online: http://www.jennajacobs.org/R/rarefaction.html (accessed on November 2019).
30. Oksanen, J.; Kindt, R.; Legendre, P.; O'Hara, B.; Stevens, M.H.H.; Oksanen, M.J. The vegan package. *Commun. Ecol. Package* **2007**, *10*, 631–637.
31. David, B.; McNiven, J. *The Oxford Handbook of the Archaeology and Anthropology of Rock Art*; Oxford University Press: Oxford, UK, 2018.
32. Bonneau, A.; Staff, R.A.; Higham, T.; Brock, F.; Pearce, D.G.; Mitchell, P.J. Successfully Dating Rock Art in Southern Africa Using Improved Sampling Methods and New Characterization and Pretreatment Protocols. *Radiocarbon* **2016**, *59*, 659–677, doi:10.1017/rdc.2016.69.
33. Zerboni, A.; Degli Esposti, M.; Wu, Y.-L.; Brandolini, F.; Mariani, G.S.; Villa, F.; Lotti, P.; Cappitelli, F.; Sasso, M.; Rizzi, A.; et al. Age, palaeoenvironment, and preservation of prehistoric petroglyphs on a boulder in the oasis of Salut (Northern Sultanate of Oman). *Quat. Int.* **2019**, doi:10.1016/j.quaint.2019.06.040.

34. Chalmin, E.; Castets, G.; Delannoy, J.-J.; David, B.; Barker, B.; Lamb, L.; Soufi, F.; Pairis, S.; Cersoy, S.; Martinetto, P.; et al. Geochemical analysis of the painted panels at the "Genyornis" rock art site, Arnhem Land, Australia. *Quat. Int.* **2017**, *430*, 60–80, doi:10.1016/j.quaint.2016.04.003.
35. Krinsley, D.H.; Dorn, R.I.; Digregorio, B.E.; Langworthy, K.A.; Ditto, J. Rock varnish in New York: An accelerated snapshot of accretionary processes. *Geomorphology* **2012**, *138*, 339–351, doi:10.1016/j.geomorph.2011.09.022.
36. Krinsley, D.H.; Digregorio, B.; Dorn, R.I.; Razink, J.; Fisher, R. Mn-Fe-Enhancing Budding Bacteria in Century-Old Rock Varnish, Erie Barge Canal, New York. *J. Geol.* **2017**, *125*, 317–336, doi:10.1086/691147.
37. Lang-Yona, N.; Maier, S.; Macholdt, D.S.; Müller-Germann, I.; Yordanova, P.; Rodríguez-Caballero, E.; Jochum, K.P.; Al-Amri, A.; Andreae, M.O.; Fröhlich-Nowoisky, J.; et al. Insights into microbial involvement in desert varnish formation retrieved from metagenomic analysis. *Environ. Microbiol. Rep.* **2018**, *10*, 264–271, doi:10.1111/1758-2229.12634.
38. Gorbushina, A. Live on the rocks. *Environ. Microbiol*. **2007**, *9*, 1613–1631.
39. Konhauser, K.; Fyfe, W.S.; Schultze-Lam, S.; Ferris, F.G.; Beveridge, T.J. Iron phosphate precipitation by epilithic microbial biofilms in Arctic Canada. *Can. J. Earth Sci.* **1994**, *31*, 1320–1324, doi:10.1139/e94-114.
40. Larson, P.H.; Dorn, R.I. Painting Yosemite Valley: A Case Study of Rock Coatings Encountered at Half Dome. *Phys. Geogr.* **2012**, *33*, 165–182, doi:10.2747/0272-3646.33.2.165.
41. Marnocha, C.L.; Dixon, J.C. Endolithic bacterial communities in rock coatings from Kärkevagge, Swedish Lapland. *FEMS Microbiol. Ecol.* **2014**, *90*, 533–542, doi:10.1111/1574-6941.12415.
42. Schabereiter-Gurtner, C.; Saiz-Jimenez, C.; Piñar, G.; Lubitz, W.; Rã¶lleke, S.; Rölleke, S. Phylogenetic diversity of bacteria associated with Paleolithic paintings and surrounding rock walls in two Spanish caves (LlonÃn and La Garma). *FEMS Microbiol. Ecol.* **2004**, *47*, 235–247, doi:10.1016/s0168-6496(03)00280-0.
43. Irit, N.; Hana, B.; Yifat, B.; Esti, K.-W.; Ariel, K. Insights into bacterial communities associated with petroglyph sites from the Negev Desert, Israel. *J. Arid. Environ.* **2019**, *166*, 79–82, doi:10.1016/j.jaridenv.2019.04.010.
44. Nir, I.; Barak, H.; Kramarsky-Winter, E.; Kushmaro, A. Seasonal diversity of the bacterial communities associated with petroglyphs sites from the Negev Desert, Israel. *Ann. Microbiol.* **2019**, *69*, 1079–1086, doi:10.1007/s13213-019-01509-z.
45. Roldán, C.; Murcia-Mascaros, S.; López-Montalvo, E.; Vilanova, C.; Porcar, M. Proteomic and metagenomic insights into prehistoric Spanish Levantine Rock Art. *Sci. Rep.* **2018**, *8*, 10011, doi:10.1038/s41598-018-28121-6.
46. Gonzalez, I.; Laiz, L.; Hermosin, B.; Caballero, B.; Incerti, C.; Saiz-Jimenez, C. Bacteria isolated from rock art paintings: The case of Atlanterra shelter (South Spain). *J. Microbiol. Methods* **1999**, *36*, 123–127, doi:10.1016/s0167-7012(99)00017-2.
47. Laiz, L.; Hermosin, B.; Caballero, B.; Saiz-Jimenez, C. Bacteria isolated from the rocks supporting prehistoricpaintings in two shelters from Sierra de Cazorla, Jaen, Spain. *Aerobiologia* **2000**, *16*, 119–124, doi:10.1023/a:1007684904350.
48. Zhang, C.; Li, F.; Lv, J. Morphology and formation mechanism in precipitation of calcite induced by *Curvibacter lanceolatus* strain HJ-1. *J. Cryst. Growth* **2017**, *478*, 96–101, doi:10.1016/j.jcrysgro.2017.08.019.
49. Kakoti, N.; Buragohain, M.; Sarmah, P.; Pegu, B.K. Arsenic Resistance Bacteria in Groundwater: A Review. *Int. Res. J. Biological. Sci*. **2020**, *9*, 47–49.
50. Di Rienzi, S.; Sharon, I.; Wrighton, K.C.; Koren, O.; Hug, L.A.; Thomas, B.C.; Goodrich, J.K.; Bell, J.T.; Spector, T.D.; Banfield, J.F.; et al. The human gut and groundwater harbor non-photosynthetic bacteria belonging to a new candidate phylum sibling to Cyanobacteria. *eLife* **2013**, *2*, 1–25, doi:10.7554/elife.01102.
51. Weiss, J.V.; Rentz, J.A.; Plaia, T.; Neubauer, S.C.; Merrill-Floyd, M.; Lilburn, T.; Bradburne, C.; Megonigal, J.P.; Emerson, D. Characterization of Neutrophilic Fe(II)-Oxidizing Bacteria Isolated from the Rhizosphere of Wetland Plants and Description of *Ferritrophicum radicicola* gen. nov. sp. nov., and *Sideroxydans paludicola* sp. nov. *Geomicrobiol. J.* **2007**, *24*, 559–570.
52. Mendoza, M.L.Z.; Lundberg, J.; Ivarsson, M.; Campos, P.; Nylander, J.A.A.; Sallstedt, T.; Dalen, L. Metagenomic Analysis from the Interior of a Speleothem in Tjuv-Ante's Cave, Northern Sweden. *PLoS ONE* **2016**, *11*, e0151577, doi:10.1371/journal.pone.0151577.
53. Perry, T.D.; Klepac-Ceraj, V.; Zhang, X.V.; McNamara, C.J.; Polz, M.F.; Martin, S.T.; Berke, N.; Mitchell, R. Binding of Harvested Bacterial Exopolymers to the Surface of Calcite. *Environ. Sci. Technol.* **2005**, *39*, 8770–8775, doi:10.1021/es0508368.

54. Konhauser, K.; Riding, R. Bacterial Biomineralization. In *Fundamentals of Geobiology*; Wiley: Hoboken, NJ, USA, 2012; pp. 105–130.
55. Urzì, C. Biomineralization Processes on Rock and Monument Surfaces Observed in Field and in Laboratory Conditions. *Geomicrobiol. J.* **1999**, *16*, 39–54, doi:10.1080/014904599270730.
56. Jroundi, F.; Schiro, M.; Ruiz-Agudo, E.; Elert, K.; Martín-Sánchez, I.; Gonzalez-Muñoz, M.T.; Rodriguez-Navarro, C. Protection and consolidation of stone heritage by self-inoculation with indigenous carbonatogenic bacterial communities. *Nat. Commun.* **2017**, *8*, 279, doi:10.1038/s41467-017-00372-3.
57. Perito, B.; Marvasi, M.; Barabesi, C.; Mastromei, G.; Bracci, S.; Vendrell, M.; Tiano, P. A Bacillus subtilis cell fraction (BCF) inducing calcium carbonate precipitation: Biotechnological perspectives for monumental stone reinforcement. *J. Cult. Herit.* **2014**, *15*, 345–351, doi:10.1016/j.culher.2013.10.001.
58. Soffritti, I.; Accolti, D.; Lanzoni, L.; Volta, A.; Bisi; Mazzacane, S.; Caselli, E.; D'Accolti, M.; Bisi, M. The Potential Use of Microorganisms as Restorative Agents: An Update. *Sustainability* **2019**, *11*, 3853, doi:10.3390/su11143853.
59. Fishman, M.R.; Giglio, K.; Fay, D.; Filiatrault, M.J. Physiological and genetic characterization of calcium phosphate precipitation by *Pseudomonas* species. *Sci. Rep.* **2018**, *8*, 10156, doi:10.1038/s41598-018-28525-4.
60. Adetutu, E.; Thorpe, K.; Shahsavari, E.; Bourne, S.; Cao, X.; Fard, R.; Kirby, G.; Ball, A.S. Bacterial community survey of sediments at Naracoorte Caves, Australia. *Int. J. Speleol.* **2012**, *41*, 137–147, doi:10.5038/1827-806x.41.2.2.
61. Han, Z.; Yu, W.; Zhao, H.; Zhao, Y.; Tucker, M.E.; Yan, H. The Significant Roles of Mg/Ca Ratio, Cl^- and $SO42^-$ in Carbonate Mineral Precipitation by the Halophile *Staphylococcus epidermis* Y2. *Minerals* **2018**, *8*, 594.
62. Marnocha, C.L.; Dixon, J.C. Bacterially facilitated rock-coating formation as a component of the geochemical budget in cold climates: An example from Kärkevagge, Swedish Lapland. *Geomorphology* **2014**, *218*, 45–51, doi:10.1016/j.geomorph.2013.07.013.
63. Rusznyák, A.; Akob, D.M.; Nietzsche, S.; Eusterhues, K.; Totsche, K.U.; Neu, T.R.; Frosch, T.; Popp, J.; Keiner, R.; Geletneky, J.; et al. Calcite Biomineralization by Bacterial Isolates from the Recently Discovered Pristine Karstic Herrenberg Cave. *Appl. Environ. Microbiol.* **2011**, *78*, 1157–1167, doi:10.1128/AEM.06568-11.
64. Maciejewska, M.; Adam, D.; Naômé, A.; Martinet, L.; Tenconi, E.; Całusińska, M.; Delfosse, P.; Hanikenne, M.; Baurain, D.; Compère, P.; et al. Assessment of the Potential Role of *Streptomyces* in Cave Moonmilk Formation. *Front. Microbiol.* **2017**, *8*, 8, doi:10.3389/fmicb.2017.01181.
65. Viti, C.; Pace, A.; Giovannetti, L. Characterization of Cr(VI)-Resistant Bacteria Isolated from Chromium-Contaminated Soil by Tannery Activity. *Curr. Microbiol.* **2003**, *46*, 1–5, doi:10.1007/s00284-002-3800-z.
66. Barns, S.M.; Cain, E.C.; Sommerville, L.; Kuske, C.R. Acidobacteria Phylum Sequences in Uranium-Contaminated Subsurface Sediments Greatly Expand the Known Diversity within the Phylum. *Appl. Environ. Microbiol.* **2007**, *73*, 3113–3116, doi:10.1128/aem.02012-06.
67. Marzan, L.W.; Hossain, M.; Mina, S.A.; Akter, Y.; Chowdhury, A.M.A. Isolation and biochemical characterization of heavy-metal resistant bacteria from tannery effluent in Chittagong city, Bangladesh: Bioremediation viewpoint. *Egypt. J. Aquat. Res.* **2017**, *43*, 65–74, doi:10.1016/j.ejar.2016.11.002.
68. Crespo-Piazuelo, D.; Estellé, J.; Revilla, M.; Mesas, L.C.; Ramayo-Caldas, Y.; Óvilo, C.; Fernández, A.I.; Ballester, M.; Folch, J.M. Characterization of bacterial microbiota compositions along the intestinal tract in pigs and their interactions and functions. *Sci. Rep.* **2018**, *8*, 12727, doi:10.1038/s41598-018-30932-6.
69. Takamatsu, D.; Ide, H.; Osaki, M.; Sekizaki, T. Identification of *Facklamia sourekii* from a Lactating Cow. *J. Vet. Med. Sci.* **2006**, *68*, 1225–1227, doi:10.1292/jvms.68.1225.
70. Atienzar, A.I.C.; Gerber, P.F.; Opriessnig, T. Use of the rSpaA415 antigen indicates low rates of *Erysipelothrix rhusiopathiae* infection in farmed cattle from the United States of America and Great Britain. *BMC Vet. Res.* **2019**, *15*, 388, doi:10.1186/s12917-019-2147-7.
71. Barton, H.; Taylor, N.; Kreate, M.; Springer, A.; Oehrle, S.; Bertog, J. The impact of host rock geochemistry on bacterial community structure in oligotrophic cave environments. *Int. J. Speleol.* **2007**, *36*, 93–104, doi:10.5038/1827-806x.36.2.5.
72. Cotta, M.; Whitehead, T.R.; Collins, M.D.; Lawson, P.A. *Atopostipes suicloacale* gen. nov., sp. nov., isolated from an underground swine manure storage pit. *Anaerobe* **2004**, *10*, 191–195, doi:10.1016/j.anaerobe.2004.04.001.

73. Wadud, S.; Michaelsen, A.; Gallagher, E.; Parcsi, G.; Zemb, O.; Stuetz, R.M.; Manefield, M. Bacterial and fungal community composition over time in chicken litter with high or low moisture content. *Br. Poult. Sci.* **2012**, *53*, 561–569, doi:10.1080/00071668.2012.723802.
74. Hanchi, H.; Mottawea, W.; Sebei, K.; Hammami, R. The Genus *Enterococcus*: Between Probiotic Potential and Safety Concerns—An Update. *Front. Microbiol.* **2018**, *9*, 9, doi:10.3389/fmicb.2018.01791.
75. Franz, C.M.A.P.; Van Belkum, M.J.; Holzapfel, W.H.; Abriouel, H.; Gálvez, A. Diversity of enterococcal bacteriocins and their grouping in a new classification scheme. *FEMS Microbiol. Rev.* **2007**, *31*, 293–310, doi:10.1111/j.1574-6976.2007.00064.x.